

# Optical modulation of aqueous metamaterial properties at large scale

Sui Yang,<sup>1,2</sup> Yuan Wang,<sup>1,2</sup> Xingjie Ni,<sup>1</sup> and Xiang Zhang<sup>1,2,3,\*</sup>

<sup>1</sup>NSF Nano-scale Science and Engineering Center (NSEC), 3112 Etcheverry Hall, University of California at Berkeley, Berkeley, California 94720, USA

<sup>2</sup>Materials Sciences Division, Lawrence Berkeley National Laboratory, 1 Cyclotron Road, Berkeley, California 94720, USA

<sup>3</sup>Department of Physics, King Abdulaziz University, Jeddah, 21589, Saudi Arabia  
[\\*xiang@berkeley.edu](mailto:xiang@berkeley.edu)

**Abstract:** Dynamical control of metamaterials by adjusting their shape and structures has been developed to achieve desired optical functionalities and to enable modulation and selection of spectra responses. However it is still challenging to realize such a manipulation at large scale. Recently, it has been shown that the desired high (or low) symmetry metamaterials structure in solution can be self-assembled under external light stimuli. Using this approach, we systematically investigated the optical controlling process and report here a dynamical manipulation of magnetic properties of metamaterials. Under external laser excitations, we demonstrated that selected magnetic properties of metamaterials can be tuned with the freedom of chosen wavelength ranges. The magnetic dipole selectivity and tunability were further quantified by in situ spectral measurement.

©2015 Optical Society of America

**OCIS codes:** (160.3918) Metamaterials; (160.4760) Optical properties.

---

## References and links

1. Y. Liu and X. Zhang, "Metamaterials: a new frontier of science and technology," *Chem. Soc. Rev.* **40**(5), 2494–2507 (2011).
2. D. R. Smith, J. B. Pendry, and M. C. K. Wiltshire, "Metamaterials and negative refractive index," *Science* **305**(5685), 788–792 (2004).
3. A. N. Grigorenko, A. K. Geim, H. F. Gleeson, Y. Zhang, A. A. Firsov, I. Y. Khrushchev, and J. Petrovic, "Nanofabricated media with negative permeability at visible frequencies," *Nature* **438**(7066), 335–338 (2005).
4. N. Fang, H. Lee, C. Sun, and X. Zhang, "Sub-diffraction-limited optical imaging with a silver superlens," *Science* **308**(5721), 534–537 (2005).
5. Z. Jacob, L. V. Alekseyev, and E. Narimanov, "Optical Hyperlens: Far-field imaging beyond the diffraction limit," *Opt. Express* **14**(18), 8247–8256 (2006).
6. R. A. Shelby, D. R. Smith, and S. Schultz, "Experimental verification of a negative index of refraction," *Science* **292**(5514), 77–79 (2001).
7. T. J. Yen, W. J. Padilla, N. Fang, D. C. Vier, D. R. Smith, J. B. Pendry, D. N. Basov, and X. Zhang, "Terahertz magnetic response from artificial materials," *Science* **303**(5663), 1494–1496 (2004).
8. S. Zhang, W. Fan, N. C. Panoiu, K. J. Malloy, R. M. Osgood, and S. R. J. Brueck, "Experimental demonstration of near-infrared negative-index metamaterials," *Phys. Rev. Lett.* **95**(13), 137404 (2005).
9. G. Dolling, C. Enkrich, M. Wegener, C. M. Soukoulis, and S. Linden, "Simultaneous negative phase and group velocity of light in a metamaterial," *Science* **312**(5775), 892–894 (2006).
10. J. Yao, Z. Liu, Y. Liu, Y. Wang, C. Sun, G. Bartal, A. M. Stacy, and X. Zhang, "Optical negative refraction in bulk metamaterials of nanowires," *Science* **321**(5891), 930 (2008).
11. J. Valentine, S. Zhang, T. Zentgraf, E. Ulin-Avila, D. A. Genov, G. Bartal, and X. Zhang, "Three-dimensional optical metamaterial with a negative refractive index," *Nature* **455**(7211), 376–379 (2008).
12. J. A. Fan, C. Wu, K. Bao, J. Bao, R. Bardhan, N. J. Halas, V. N. Manoharan, P. Nordlander, G. Shvets, and F. Capasso, "Self-Assembled Plasmonic Nanoparticle Clusters," *Science* **328**(5982), 1135–1138 (2010).
13. S. Vignolini, N. A. Yufa, P. S. Cunha, S. Guldin, I. Rushkin, M. Stefik, K. Hur, U. Wiesner, J. J. Baumberg, and U. Steiner, "A 3D Optical Metamaterial Made by Self-Assembly," *Adv. Mater.* **24**(10), OP23–OP27 (2012).
14. A. Kuzyk, R. Schreiber, Z. Fan, G. Pardatscher, E.-M. Roller, A. Högele, F. C. Simmel, A. O. Govorov, and T. Liedl, "DNA-based self-assembly of chiral plasmonic nanostructures with tailored optical response," *Nature* **483**(7389), 311–314 (2012).

15. S. Yang, X. Ni, X. Yin, B. Kante, P. Zhang, J. Zhu, Y. Wang, and X. Zhang, "Feedback-driven self-assembly of symmetry-breaking optical metamaterials in solution," *Nat. Nanotechnol.* **9**(12), 1002–1006 (2014).
16. H. T. Chen, J. F. O'Hara, A. K. Azad, A. J. Taylor, R. D. Averitt, D. B. Shrekenhamer, and W. J. Padilla, "Experimental demonstration of frequency-agile terahertz metamaterials," *Nat. Photonics* **2**(5), 295–298 (2008).
17. M. J. Dicken, K. Aydin, I. M. Pryce, L. A. Sweatlock, E. M. Boyd, S. Walavalkar, J. Ma, and H. A. Atwater, "Frequency tunable near-infrared metamaterials based on VO<sub>2</sub> phase transition," *Opt. Express* **17**(20), 18330–18339 (2009).
18. M. Liu, H. Y. Hwang, H. Tao, A. C. Strikwerda, K. Fan, G. R. Keiser, A. J. Sternbach, K. G. West, S. Kittiwatanakul, J. Lu, S. A. Wolf, F. G. Omenetto, X. Zhang, K. A. Nelson, and R. D. Averitt, "Terahertz-field-induced insulator-to-metal transition in vanadium dioxide metamaterial," *Nature* **487**(7407), 345–348 (2012).
19. V. E. Ferry, J. M. Smith, and A. P. Alivisatos, "Symmetry Breaking in Tetrahedral Chiral Plasmonic Nanoparticle Assemblies," *ACS Photonics* **1**(11), 1189–1196 (2014).
20. V. N. Smolyaninova, B. Yost, D. Lahnehan, E. E. Narimanov, and I. I. Smolyaninov, "Self-assembled tunable photonic hyper-crystals," *Sci. Rep.* **4**, 5706 (2014).
21. A. Kuzyk, R. Schreiber, H. Zhang, A. O. Govorov, T. Liedl, and N. Liu, "Reconfigurable 3D plasmonic metamolecules," *Nat. Mater.* **13**(9), 862–866 (2014).
22. B. Nikoobakht and M. A. El-Sayed, "Preparation and growth mechanism of gold nanorods (NRs) using seed-mediated growth method," *Chem. Mater.* **15**(10), 1957–1962 (2003).
23. C. J. Murphy, T. K. Sau, A. M. Gole, C. J. Orendorff, J. Gao, L. Gou, S. E. Hunyadi, and T. Li, "Anisotropic metal nanoparticles: Synthesis, assembly, and optical applications," *J. Phys. Chem. B* **109**(29), 13857–13870 (2005).
24. P. K. Jain, W. Qian, and M. A. El-Sayed, "Ultrafast cooling of photoexcited electrons in gold nanoparticle-thiolated DNA conjugates involves the dissociation of the gold-thiol bond," *J. Am. Chem. Soc.* **128**(7), 2426–2433 (2006).
25. M. Reisman, J. C. Bretschneider, G. von Plessen, and U. Simon, "Reversible photothermal melting of DNA in DNA-gold-nanoparticle networks," *Small* **4**(5), 607–610 (2008).
26. J. B. Pendry, D. Schurig, and D. R. Smith, "Controlling electromagnetic fields," *Science* **312**(5781), 1780–1782 (2006).
27. W. S. Cai, U. K. Chettiar, A. V. Kildishev, and V. M. Shalaev, "Optical cloaking with metamaterials," *Nat. Photonics* **1**(4), 224–227 (2007).

## 1. Introduction

Metamaterials are designed artificial composites whose properties are primarily from their structures rather than chemical compositions [1]. With their constituent "meta-atoms" tailored at a sub-wavelength scale, metamaterials have opened the exciting gateway to reach extraordinary properties and applications such as artificial magnetic activities, negative refraction and deep-subwavelength imaging [2–5]. The route to metamaterials has traditionally taken a top-down fabrication technology such as Focus Ion Beam (FIB) and Electron Beam Lithography (EBL). In the past decade, we have indeed seen tremendous research advancement that has brought metamaterials responses from microwave to optical frequency [6–11]. Recently, metamaterials fabrication can also be realized by the state-of-the-art self-assembly methods offering better spatial resolution and large scalability [12–15]. However, the dynamically controllable tuning of the structures and properties metamaterials at a large scale still remains challenge.

Frequency tunability of metamaterials using top-down fabrication technique, for example, was demonstrated by switching an intrinsic semiconductor to metal either through photo-carrier generation under strong ultrashort laser pulse irradiations [16] or using a phase change materials such as vanadium dioxide (VO<sub>2</sub>) [17,18]. Structure tunability could be offered by self-assembly techniques with combined chemical specificity and induced external stimuli [19,20]. More recently, a reconfigurable three dimensional (3D) plasmonic metamolecules was demonstrated using DNA-regulated conformational changes [21]. However, the aforementioned tuning of metamaterials still remains at single element or a few elements level.

We have previously demonstrated a feedback driven self-assembly route using external light stimuli to rather control the final desired metamaterials structures precisely [15]. However, we note that this unique developed method can be a ideal route to dynamically adjust assembled structures *on-site* in achieving desired optical functionalities and spectra selectivity. By a systematic investigation on optical controlling process, we report here the

dynamical manipulation of magnetic properties of metamaterials using previously developed feedback self-assembly mechanism. Moreover, the tunability and selectivity of magnetic responses of metamaterials have been quantified.

## 2. Fabrication and modelling

Due to its interesting structure-dependent optical properties, the metamaterial we investigate is coupled nanorod dimer system with a mutual longitudinal offset (position displacement) that enriches its optical modes [15]. Gold nanorods were prepared by using a seed mediated growth method [22,23]. The assembly of nanorod pairs involves the control of the hydrophobation of gold nanorods and the interfacial-preferential binding (Fig. 1(a)). Typically, the fresh prepared gold nanorods was centrifuged by disposal of excess Cetyltrimethylammonium bromide (CTAB) and washed 2:1(v/v) water/chloroform solution by extraction. After discarding the chloroform layer, the gold nanorod suspension was quickly added to a 3  $\mu$ L mercaptopropyltrimethoxysilane (MPS) solution in ethanol (1mM) (designed for pronounced offset  $\sim$ 20nm, adding more MPS will result in different level of hydrophobation and thus offsets). During the stirring of this mixture, gold nanorod particles were incubated by adding 1 ml of an octadecyltrimethoxysilane (ODS) chloroform solution (1:1000 (v/v)) and 10  $\mu$ L sodium hydroxide NaOH (1M) to achieve surface functionalization. Dimer assembly was performed by dropwise introduction of disodium chromoglycate (DSCG) solution with a concentration of 500  $\mu$ M when the nanorods stabilized at water-chloroform interface (light red color observed at the interlayer). An offset along the longitudinal side is created due to the hydrophobation of lateral nanorod surface deprived of CTAB. After assembly, the solution near the interlayer was taken out and purified several times with ultrafiltration centrifugal nanosep devices containing membranes of 0.035  $\mu$ m and 0.45  $\mu$ m to remove large clusters.

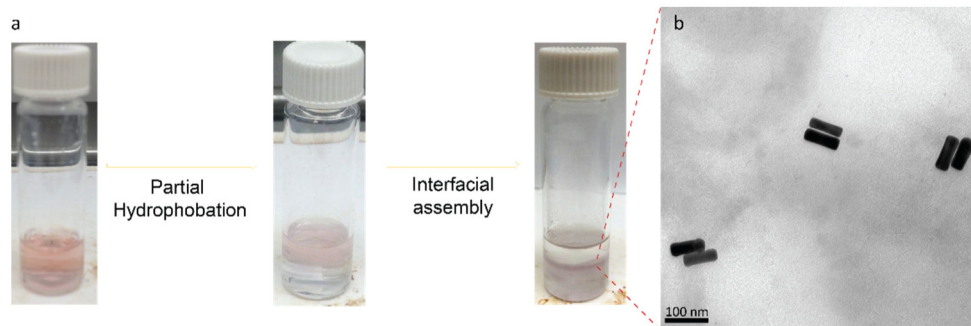


Fig. 1. (a) The experimental pictures illustrating the two processes of coupled nanorod assembly involving partial hydrophobation and preferential interface assembly. (b) Transmission electron microscopy (TEM) image of assembled gold nanorod dimers showing typical offsets along longitudinal axis.

The result of of dimer assembly shows that coupled nanorod pairs were successfully synthesized with longitudinal offsets along the side (Fig. 1(b)). For detailed analysis, we have performed the structural statistical measurement (over 100 dimer particles) along with the theoretical spectra calculations performed by CST Microwave Studio. The decomposed spectra result of the sample is shown in Fig. 2. The intensity differences in spectra are from distinct populations of dimers with various offsets estimated from structure statistics. Due to the unique structure-dependent optical responses, we could dynamically reconfigure our metamaterial structures by recently developed plasmon-mediated feedback mechanism using external light control [14]. The designed working window of wavelength ( $\lambda$ )  $\sim$ 760-930nm as shown is chosen because of the effectiveness of structural re-population.

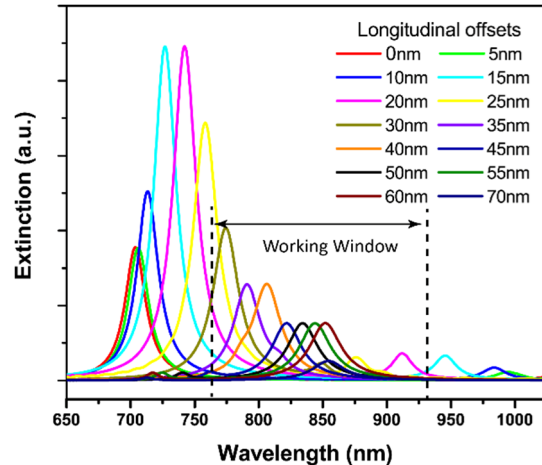


Fig. 2. The decomposed extinction spectra using experimental structural statistics (various offsets' populations) along with theoretical spectra simulations (polarization along longitudinal direction of dimers) with 5nm increment step of dimers offsets. Large peak in each decomposed spectrum is electric dipole response while the smaller peak corresponds to magnetic dipole resonance.

### 3. Experiment and discussion

With the detailed information on structural statistics and modes dispersion, we were able to tuning the metamaterials responses selectively and dynamically. A schematic of the assembly and optical setup is shown in Fig. 3(a). Similar to a pump and probe experiment, a laser light was used to excite the metamaterials structures in solution while a white light source was illuminated through the sample to monitor the spectra. Under laser light excitation as shown, plasmon resonances are induced at nanodimers in the way that only dimers with the right shift (offset) will survive while other “undesired” shifted structures will be disassembled due to the photothermal heating from the plasmon resonances [24,25]. Meantime, the disassembled nanorods could reassemble into dimers because of the presence of bonding molecules in solution. And the reassembly of dimers prefers to form the right amount of offset because the illumination prevents them to recombine into “undesired” offsets. Using such a feedback mechanism, the structures and properties of metamaterials can be dynamically controlled. In a typical experiment, 200  $\mu\text{L}$  as-assembled dimer metamaterial solution in quartz cuvette was irradiated by Femtosecond laser (laser pulse duration: 100 fs) with designed working range of wavelength ( $0.875 \text{ kWcm}^{-2}$  average power density). The total number dimer particles affected by the laser illumination is estimated on the order of  $10^7$ . The course of dynamical tuning process was monitored in situ by measuring transmission spectroscopy via white light exposure.

To clear illustrate the effectiveness and dynamical properties manipulation process, we have performed a series of scanning windows in designed working wavelength range. The dynamical tuning of metamaterial magnetic response is clearly demonstrated in measured extinction spectra (Fig. 3(b)). Starting from as-made dimer metamaterials (red), the spectra were measured at a variety of laser excitation wavelength ranges at an extending interval of 40 or 50 nm. As increasing the scanning window, the gradual narrowing and re-shaping of metamaterial response was observed and the ensemble resonance peak changed from asymmetric to symmetric. This could be a result of reconfiguration of the dimer metamaterials structure due to the structural homogenization process by selective excitation of plasmon resonances. Gradually, a small hump with broad linewidth was emerged at  $\lambda$  between 900 and 1000 nm, which can be ascribed to ensemble magnetic dipole resonance (M) from highly populated dimers with designed offset between 10 and 20 nm (Fig. 2). This

emerging magnetic feature further confirms that metamaterials structures are dynamically reshaping at a higher selectivity. The magnetic response reaches the maximum with a narrower linewidth observed at scan window 930-760nm. At the same time, the electric dipole resonance ( $\lambda$  between 700 and 800 nm) become symmetric and shows a trend of blue-shifting as extending illumination window. As shown, by designing and scanning wavelength windows dynamically, we can achieve not only the desired magnetic functionality of metamaterials, but also the tuning of response strength and linewidth.

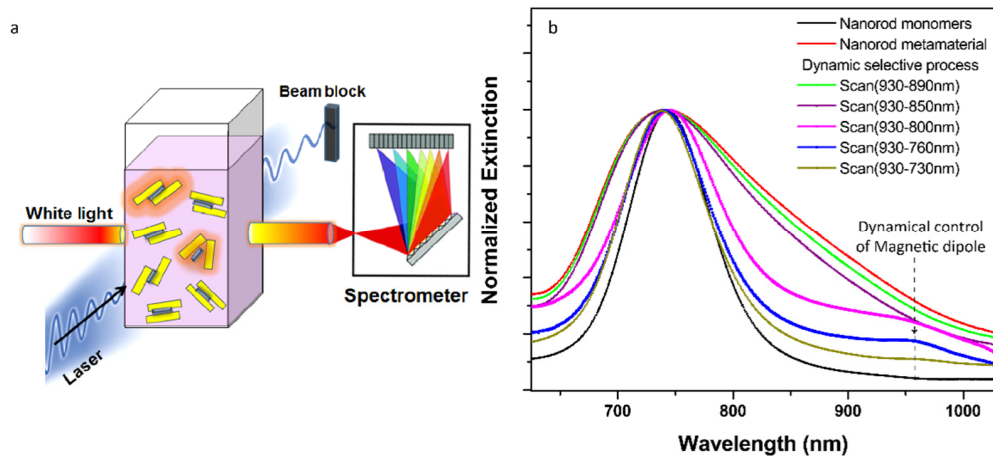


Fig. 3. Dynamical manipulation of magnetic properties of assembled nanorod dimer metamaterials. (a) Schematic sketch of the assembly and optical setup. The sample was exposed with Ti-Sapphire laser in different wavelength ranges and spectra was monitored via orthogonal white light illumination channel. (b) Experiment measured extinction spectra of sample after illumination at different wavelength ranges. A clear ensemble magnetic dipole feature has gradually evolved as a result of structural homogenization (see Visualization 1). The dotted arrow lines is guided for the position of magnetic dipole response and its evolvement. Different colors present laser illumination at different wavelength ranges with monomers (black) and as-made dimers (red) for comparison.

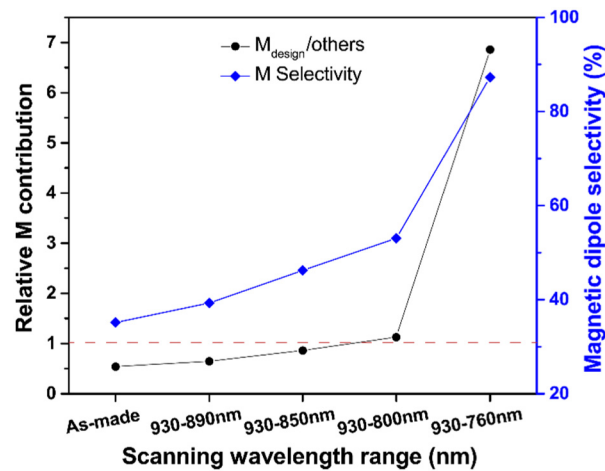


Fig. 4. Quantification of desired magnetic dipole response. The relative contribution of desired magnetic (M) response (left axis) and selectivity (right axis) are plotted as a function of laser scanning wavelength ranges. The dotted line is guided for turning point of relative M contribution for having distinct ensemble magnetic spectral responses.

The tunability of metamaterials responses was further quantified by extracting contributions from the emerging (designed) magnetic dipole resonance by area integration of the resonance peak (910-990 nm). The selectivity and relative contributions is defined as the ratio between the integral of designed magnetic dipole response with respect to the total and other dipoles contributions at long wavelength region (880-1025 nm) due to the inhomogeneous broadening effect. As shown, we have achieved high degree of tunability of magnetic properties with highest selectivity as much as  $\sim 90\%$  (Fig. 4). Interestingly, both magnetic dipole (M) contributions and selectivity show a threshold-like growing trend as extending laser excitation window. The turning point is at the range scanned from 930 to 800 nm, which is corresponding to the relative M contribution value of 1.13 (just above one). Note that the magnetic feature (designed) just start to show up in measured extinction spectrum at this scanning window (Fig. 2(b)). It can be inferred that critical requirement of having distinct ensemble magnetic spectral resonance is to achieve relative M contribution value greater than one. This quantitative information enables designing and selecting spectral responses of metamaterials to achieve desired optical functionalities. A clear Lorentzian function of estimated effective permeability is presented at the magnetic dipole resonance (Fig. 5). As shown, it presents a highly tunable effective permeability with respect to both wavelength and filling factor at optical frequency. The manipulation of such effective behaviors of metamaterial could result in astonishing achievements such as optical cloaking [26] and transformation optics [27].

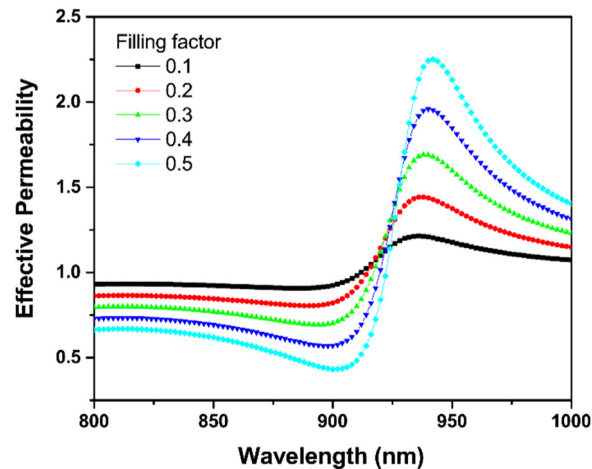


Fig. 5. Theoretical retrieval of effective permeability (real part) as a function of wavelength with respect to filling factor.

#### 4. Conclusions

In summary, we have experimentally demonstrated the dynamical manipulation of optical properties of metamaterials in solution. By in situ monitoring the extinction spectra, we have also quantified the tunability and selectivity of magnetic dipolar responses. Such a dynamical approach could provide new opportunities in tailoring and developing active and reconfigurable optical devices and novel optical applications.

#### Acknowledgments

This research was supported by the National Science Foundation (Grant no. DMR-1344290) and the Gordon and Betty Moore Foundation.